JMBFS

Journal of Microbiology, Biotechnology and Food Sciences

International peer-reviewed scientific online journal

Published by Faculty of Biotechnology and Food Sciences

NOMOGRAMS FOR DETERMINING THE THERMO-PHYSICAL PROPERTIES OF FRUIT JUICES

Oybek Ismailov[1], Doniyor Ganijonov[2], Fozilbek Shomansurov[1], To'ychi Pirimov[2], Ganisher Rakhimov[3]*

Address(es):

[1] Institute of General and Inorganic Chemistry, Academy of Sciences of the Republic of Uzbekistan, 77[a] Mirzo-Ulugbek Ave.,100170, Tashkent, Uzbekistan, phone number: +(99871) 262-56-60, 262-79-90.

[2] Gulistan State University (GulSU), Gulistan city 4 microdistrict, Gulistan, Uzbekistan, phone number: +(0367) 225-02-75.

[3] Qarshi State Technical University, 180100 / 180119, Qarshi, Uzbekistan, phone number: +(99875) 220-09-24.

*Corresponding author: ismailovnmpi@mail.ru

https://doi.org/10.55251/jmbfs.12745

ARTICLE INFO

Received 29. 4. 2025
Revised 12. 11. 2025
Accepted 24. 11. 2025
Published 1. 12. 2025

Regular article

OPEN ACCESS

ABSTRACT

Accurate thermophysical property data are indispensable for heat-transfer calculations, equipment sizing, and reliable control of thermal treatments in juice processing. Yet these properties depend jointly on temperature and soluble-solids content and can vary by cultivar, creating a gap between laboratory tabulations and day-to-day engineering needs. This study quantifies those dependencies for directly pressed apple juices from the Golden Rangers and Simirenko cultivars and introduces compact nomograms that enable rapid, instrument-free estimation of key properties during design and operation.

Experimental measurements covered density (kg·m^{-3}), kinematic viscosity (mm^2·s^{-1}), thermal conductivity (W·m^{-1}·K^{-1}), and specific heat capacity (kJ·kg^{-1}·K^{-1}) across 20–90 °C and soluble-solids levels of 12–15%. The soluble-solids content in the tested juices was 12.7–14.3%, corresponding to 11.5–13 °Brix, consistent with single-strength apple juice. Nomograms were constructed from the experimental surfaces using separable temperature–solids mappings to ensure linear, parallel scales for temperature, solids, and the target property, providing accurate read-off within the measured domain.

The data show that, within the studied range, higher soluble-solids content produces an average 3.2% rise in density. At 20 °C, kinematic viscosity was 1.45 mm^2·s^{-1} for Golden Rangers and 1.38 mm^2·s^{-1} for Simirenko; heating from 20 to 90 °C reduced viscosity by up to a factor of 3.1. Increasing soluble solids from 12% to 15% decreased thermal conductivity by up to 3.2%, whereas raising temperature from 20 to 90 °C increased specific heat capacity by about 3.7% (≈3% overall at 12.7–14.3% solids). Across compositions, specific heat varied by roughly 3–5% relative to the solids fraction.

Practically, the nomograms allow engineers to (i) interpolate properties quickly for energy and duty calculations, (ii) compute Reynolds and Prandtl numbers for heat-exchanger design and verification, and (iii) evaluate how moderate shifts in °Brix or operating temperature affect residence time and thermal load during pasteurization (notably in tubular exchangers). The tools are intended for use within the measured bounds (20–90 °C; 12–15% solids); extension to broader °Brix ranges and additional fruit matrices represents a natural avenue for future work.

Keywords: dissolved solids, density, viscosity, thermal conductivity, specific heat capacity, nomogram

INTRODUCTION

Sustained growth of the world's population continues to drive demand for safe, nutritious, and shelf-stable foods, with fruits, vegetables, and their natural juices occupying an increasingly prominent place in the human diet. Fruit juices combine high palatability with physiological value: they supply vitamins, mineral salts, amino acids, and a range of bioactive compounds that can support health maintenance and disease prevention. In addition to quenching thirst effectively, natural juices may assist detoxification processes, help regulate gastrointestinal function, contribute to lowering blood cholesterol, and modulate immune responses; importantly, they are generally low in calories and easily digestible **(Bagde et al., 2011; Gestal et al., 2004; Mullen et al., 2007)**. To maximize these benefits, juices should be prepared from fresh, ecologically clean raw materials without added preservatives or food additives. For fiber-rich fruits, producing pulpy juices is advantageous because it retains pectin substances and related colloids that are beneficial for texture and health **(Agbaje et al., 2020; Salehi 2020; Evrendilek et al., 2000)**.

Industrial juice products exhibit substantial variation in composition and properties depending on fruit species, cultivar, degree of ripeness, and processing route (direct pressing, reconstitution, or concentration and subsequent dilution) **(Deniskin et al., 2004)**. In Uzbekistan, the large-scale cultivation of fruit and vegetable crops has underpinned a steady expansion of juice production and preservation, where thermal processing remains the principal means of ensuring microbiological stability and extending shelf life. Within this context, pasteurization regimes are routinely tailored to the physical–chemical characteristics of the juice matrix, which makes reliable property data a prerequisite for rational process design and control.

From an engineering standpoint, accurate analysis of heat exchange and fluid motion in pasteurization equipment requires well-characterized thermophysical properties of the working medium. The key quantities include density (ρ), viscosity (which determines momentum transport and hydrodynamic regime), specific heat capacity (Cp), and thermal conductivity (λ). Together, these properties govern energy requirements, residence times, pressure drops, and overall heat-transfer coefficients, and therefore directly influence equipment sizing, operating parameters, and product quality outcomes **(Goren'kov et al., 2006; Makarova et al., 2012)**. Because hydrodynamic regimes (laminar, transitional, or turbulent) and the associated dimensionless groups (Reynolds, Prandtl, Nusselt numbers) depend sensitively on fluid properties, credible property correlations are essential for both design calculations and in-process verification **(Erdogdu 2005)**. In practical pasteurization lines, even modest changes in temperature or soluble-solids content can shift these regimes and alter heat-transfer efficiency **(Walkling et al., 2008)**.

Despite the abundance of data on fruit juices, property values reported in the literature are often scattered across sources, measured under differing conditions, or limited to narrow temperature or composition ranges. Moreover, cultivar-specific differences and the combined effects of temperature and soluble solids (°Brix) are not always captured in forms that are convenient for day-to-day calculations on the production floor. To bridge this gap, there is a clear need for compact, transparent tools that translate experimentally measured dependencies into a form suitable for rapid engineering use without specialized software.

The present study focuses on directly pressed apple juices from the Golden Rangers and Simirenko cultivars, which are widely cultivated and technologically relevant. The Golden Rangers cultivar is noted for its high yield (fruit mass up to 200 g; up to 600 c/ha), while Simirenko typically produces fruits up to 175 g with an average of 280 c/ha **(Bayindirli 1992)**. We investigate how temperature (20–90 °C) and mass fraction of dissolved solids (12–15 %) jointly affect four target properties - ρ (kg/m^3), ν (m^2/s), λ (W/m·K), and C_p (kJ/kg·K) - and we distill the results into nomograms that allow rapid read-off of property values as a function of temperature and composition.

The contributions of this work are twofold. First, we provide a consistent, cultivar-resolved experimental dataset across an application-relevant temperature – composition domain, ensuring internal comparability of ρ, ν, λ, and C_p under identical measurement protocols. Second, we translate these datasets into compact nomograms with parallel scales for temperature, soluble solids, and the property of interest, enabling fast, instrument-free estimation during process design and operation. These nomograms are intended for practical use in the calculation and design of tubular pasteurizers at food-processing enterprises, improving the efficiency and robustness of engineering decisions. In addition, they serve as a methodological resource in education and research, supporting calculation-and-design work by students, postgraduate researchers, and practicing engineers **(Goren'kov et al., 2006; Makarova et al., 2012; Erdogdu 2005; Walkling et al., 2008)**.

MATERIALS AND METHODS

Experiments were performed on freshly extracted juices/purees of two apple cultivars, Golden Rangers and Simirenko. Two controlled factors were varied:

- Temperature T (°C), typically from 20 to 90 °C with 10 °C increments;
- Mass fraction of dissolved solids S (%), typically 12–15 % with 1 % increments.

For each cultivar and for each thermophysical property, measurements were arranged on a rectangular (T, S) grid to obtain response tables Y (T, S), where Y denotes one of: density ρ, kinematic viscosity ν, thermal conductivity λ, or specific heat capacity C_p. All raw records were transferred to a digital spreadsheet using a dot as the decimal separator and checked for transcription errors and rare outliers. The mass fraction of dissolved solids in freshly extracted apple juices was measured by refractometry according to GOST 34128-2017 (range 2.0–80.0 %).

Density Measurement

Density (ρ, kg/m³) was measured using a 10 cm³ pycnometer following GOST 33276-2015 (±0.5 °C), across temperatures from 20°C to 90°C. Where noted for comparison and validation, the correlation reported by Bayındırlı was used: **(Magerramov et al., 2007)**:

$$\rho = 0{,}83 + 0{,}35\exp(0{,}01S) - 0{,}000564T \quad (1)$$

where T is in °C and S is the mass fraction of dissolved solids in percent.

Kinematic Viscosity

Kinematic viscosity (ν, mm² s⁻¹) was measured at 20–90 °C using a glass VPZ-4 capillary viscometer (d = 0.37 ± 0.02 mm; calibration constant K = 0.0288 mm² s⁻²). The viscosity ν was calculated from the average flow time τ_{av} (s) as **(Gasperi et al., 2009; Magerramov et al., 2006)**:

$$\nu = \frac{g}{9.807} \cdot \tau_{av} K, \quad (2)$$

where, - g is gravitational acceleration (m s⁻²); - τ_{av} is average flow time (s).

Determination of Thermal Conductivity

During the thermal processing of fruit juices, changes in the product's chemical composition, operating temperature, and pressure result in corresponding variations in thermal conductivity. As a general rule, the thermal conductivity of processed liquids increases with rising temperature. This phenomenon is largely attributed to changes in the physical (phase) state of the fluids **(Magerramov et al., 2006)**.

Thermal conductivity (λ, W m⁻¹ K⁻¹) was calculated using the empirical equation proposed by E. S. Gorenkov **(Goren'kov et al., 2006)**:

$$\lambda = 0{,}496 - 3{,}1 \cdot 10^{-3} S + 3{,}835 \cdot 10^{-5} S \cdot \mathrm{T} - 1{,}758 \cdot 10^{-5} \mathrm{T}^2 + 2{,}459 \cdot 10^{-7} S \cdot \mathrm{T}^2. \quad (3)$$

The thermal conductivity of cherry juice was determined using the mathematical equation proposed by M.A. Magerramov **(Goren'kov et al., 2006)**:

$$\lambda = \lambda_0(\mathrm{T}) - 4{,}65 \cdot 10^{-3} \cdot S + 1{,}35 \cdot 10^{-5} \cdot S^2 \quad (4)$$

Reported deviations from experiment are within ±1 % for Eq. (3) and approximately 1.5 -2 % for Eq. (4).

Determination of Specific Heat Capacity

The specific heat capacity is defined as the amount of heat required to change the temperature of a unit mass (kg) of a substance by 1 *K* without altering its phase. During the thermal processing of fruit juices, one of the most important thermal characteristics is the specific heat capacity, as it serves as a key parameter for describing heat exchange processes within processing equipment.

The specific heat capacity of fruit juices varies depending on the concentration of dissolved solids. Therefore, various researchers have conducted studies on the specific heat capacities of different fruit juices, and mathematical expressions have been derived based on experimental data (**G'anijonov et al., 2025; G'anijonov et al., 2025; G'anijonov et al., 2024.,**).

In this study, the specific heat capacity of the juice samples was determined using the equation proposed by M.A. Magerramov**.** According to this model, for apple juice with a dissolved solids mass fraction of up to 14.3%**,** the following equation is used **(Goren'kov et al., 2006; G'anijonov et al., 2025)**:

$$C_p = 3{,}722 + 2{,}010 \cdot 10^{-3} T \quad (5)$$

For cherry juice, the mass fraction of dissolved solids c =11.3%, the following mathematical formula was used to determine the specific heat capacity:

$$C_p = 3{,}811 + 1{,}919 \cdot 10^{-3} T \quad (6)$$

If the mass fraction of dissolved solids c increases up to c =18.8%**,** the following equation is used to calculate the specific heat capacity:

$$C_p = 3{,}58 + 2{,}702 \cdot 10^{-3} T \quad (7)$$

Quadratic Regression Model (for Nomogram Construction)

To obtain compact predictive relations and enable nomographic analysis, each response $Y \in \{\rho, \nu, \lambda, C_p\}$ was modeled for each cultivar by a quadratic regression without cross-term:

$$Y(t,S) = b_0 + b_1 t + b_2 S + b_3 t^2 + b_4 S^2, \quad (8)$$

where $b_0, \ldots, b_4$ are least-squares estimates. Regressions were performed in Excel (Data → Data Analysis → Regression or LINEST), using the predictor matrix $[1, t, S, t^2, S^2]$ and the measured Y as the response vector. Model adequacy was assessed by R^2, RMSE, and (where appropriate) MAPE; residuals were examined to verify the absence of systematic trends and heteroscedasticity. If diagnostics suggested underfitting, an extended model with a t, S cross-term was considered and compared by adjusted R^2 and AIC.

Transformation to Nomographic Form and Plotting

For efficient graphical determination, Eq. (8) was rewritten in additive form by introducing

$$f_1(T) = b_1 T + b_2 T^2, \qquad f_2(S) = b_2 S + b_4 S^2,$$
$$f_3(Y) = Y - b_0,$$

which yields

$$f_3 = f_1 + f_2. \quad (9)$$

This representation permits a three-scale parallel nomogram: the S-scale (left), the Y-scale (center), and the T-scale (right), all sharing a common vertical coordinate u. Let

$$a = f_2(S_{min}), \qquad b = f_1(T_{min}),$$

and choose vertical spans H_S and H_T (in mm) for the working ranges $S_{min} \to S_{max}$ and $T_{min} \to T_{max}$, respectively. The vertical scale factors are

$$m = \frac{H_S}{f_2(S_{max}) - f_2(S_{min})}, \qquad n = \frac{H_T}{f_1(T_{max}) - f_1(T_{min})}.$$

The three scales are then defined by

(left) $x = x_S$, $u = m[f_2(S) - a]$,

(center) $x = x_Y$, $u = mn/(m + n)\,[f_3(Y) - (a + b)]$,

(right) $x = x_T$, $u = n[f_1(T) - b]$,

with $x_S < x_Y < x_T$ fixed along the horizontal axis. Major/minor ticks are placed at the desired S and T values by evaluating the corresponding u. A single straight indicator line drawn through the points $(x_S,u(S))$ and $(x_T,u(T))$ intersects the central scale at (x_Y,u_Y), which yields the desired Y. The inverse problems (finding T or S for a given Y and the other factor) are solved by the same construction.

All plots were generated programmatically from the estimated coefficients to ensure a shared vertical mapping for the three scales within each nomogram (a necessary condition for geometric correctness), and to provide reproducible coordinates for ticks and labels.

The proposed procedure - experimental tabulation of $Y(T,S)$, quadratic regression (Eq. 8), and additive nomographic construction (Eq. 9) - is generic. It can be applied, without modification of the algorithm, to juices and purees of other fruit crops to develop practical nomograms for their thermophysical properties as functions of temperature and dissolved-solids concentration.

RESULTS AND DISCUSSION

Dissolved-solids determination in juice

Figure (1) show the concentrations of dissolved solids in apple juice samples from the "Golden Rangers" and "Simirenko" varieties ranged from 12.7% to 14.3% (g 100 g⁻¹ juice)

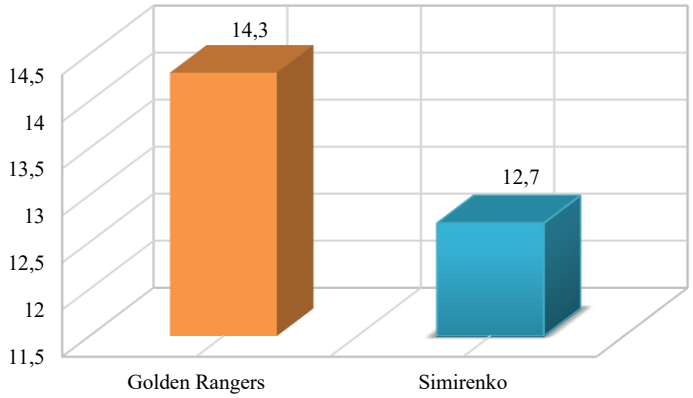

Figure 1 Dissolved-solids content (g 100 g⁻¹) of the juice samples

The sugar profile of apple juice is formed by natural sugars - fructose (4-6%), glucose (2-4%), and sucrose (1-2%); on average, about 90% of the dry-matter content consists of sugars. In our study, we analyzed juices from the Golden Rangers and Simirenko cultivars, with soluble-solids concentrations of 12.7-14.3% (g per 100 g of juice), which corresponds to 11.5-13 °Brix and agrees with literature data for single-strength juices.

Because the mass fraction of sugars correlates directly with °Brix, the density of apple juice increases with sugar content: at 10 °Brix it is about 1.038 g/cm³, whereas in concentrates with 65–68 °Brix it reaches ≈1.33 g/cm³. In the present work, the object of study was direct-pressed juice intended for pasteurization; during the experiments, the concentration of dissolved solids was kept constant. Therefore, variations in °Brix did not influence the thermophysical characteristics observed in our experiments.

Effect of temperature and dissolved-solids concentration on juice density

The density of each juice sample was measured at four dissolved-solids concentrations (12-15% w/w) and eight temperatures (20-90 °C). Data for the Golden Rangers variety are shown in Table 1; data for Simirenko are shown in (Tab 2).

Table 1 Density of "Golden Rangers" juice as a function of temperature and dissolved-solids concentration

Temperature (°C)	Mass fraction of dissolved solids (%)			
	12	13	14	15
	Density ρ, g cm⁻³			
20	1,046	1,051	1,058	1,063
30	1,045	1,05	1,057	1,062
40	1,042	1,047	1,054	1,059
50	1,037	1,042	1,049	1,054
60	1,034	1,039	1,046	1,051
70	1,026	1,031	1,038	1,043
80	1,021	1,026	1,033	1,038
90	1,015	1,019	1,027	1,031

At 20 °C, "Golden Rangers" juice density increased from 1.046 to 1.063 g cm⁻³ as solids content rose from 12% to 15% (a 1.7% increase); heating to 90 °C produced a further 2.8% increase. For "Simirenko," density at 20 °C rose from 1.042 to 1.060 g cm⁻³ over the same solids range, while heating to 90 °C caused a 2.9% decrease. Overall, increasing dissolved solids from 12% to 15% yielded an average 3.2% rise in density across both varieties. This is considered one of the critical factors influencing hydrodynamic regimes in heat exchange processes.

Table 2 Density of "Simirenko" juice as a function of temperature and dissolved-solids concentration

Temperature (°C)	Mass fraction of dissolved dry matter, %			
	12	13	14	15
	Density ρ, g/sm³			
20	1,042	1,049	1,055	1,060
30	1,040	1,047	1,053	1,058
40	1,037	1,044	1,050	1,055
50	1,031	1,038	1,043	1,048
60	1,023	1,030	1,035	1,040
70	1,020	1,028	1,032	1,038
80	1,012	1,020	1,024	1,030
90	1,008	1,016	1,020	1,025

Effect of temperature on kinematic viscosity

Table 3 Kinematic viscosity of "Golden Rangers" and "Simirenko" juices at various temperatures

Temperature (°C)	Kinematic viscosity ν (mm²/s)							
	"Golden Rangers"				"Semerenko"			
	Mass fraction of dissolved dry matter, %							
	12	13	14	15	12	13	14	15
20	1,46	1,52	1,57	1,62	1,42	1,49	1,54	1,58
30	1,43	1,48	1,54	1,59	1,36	1,43	1,48	1,53
40	1,28	1,33	1,37	1,42	1,23	1,29	1,34	1,38
50	1,16	1,20	1,24	1,29	1,15	1,21	1,25	1,29
60	1,07	1,11	1,15	1,19	1,06	1,11	1,15	1,18
70	0,97	1,00	1,04	1,07	0,95	1,00	1,04	1,07
80	0,85	0,88	0,91	0,94	0,83	0,87	0,90	0,93
90	0,73	0,75	0,78	0,81	0,71	0,74	0,77	0,79

The table 3 presents kinematic viscosity values (mm²/s) of freshly extracted apple juices as functions of temperature t (20–90 °C) and mass fraction of dissolved dry matter S (12–15%). Measurements were performed with a VPZ-4 glass capillary viscometer under thermostatic control (±0.5 °C). For each (t, S) node, the mean of 3–5 repeated measurements was used; the method's repeatability in this range is approximately 1–2% of the reading. A comma is used as the decimal separator in the table.

Across the full (t,S) grid, the kinematic viscosity ν\nuv of both apple juices exhibits smooth, monotonic, and quantitatively consistent behavior. At any fixed solids level S, ν decreases with temperature t. For "Golden Rangers," the drop at S=12% is from 1.46 mm²/s (20 °C) to 0.73 mm²/s (90 °C), and at S=15% from 1.62 to 0.81 mm²/s; for "Simirenko," the corresponding declines are 1.42 → 0.71 and 1.58 → 0.79 mm²/s. Averaged over the 20–90 °C span, this is roughly 0.10–0.12 mm²/s per 10 °C (depending on S and cultivar), reflecting the expected weakening of intermolecular cohesion and the rise of molecular mobility in aqueous sugar solutions upon heating. The temperature response is nearly linear over 20–90 °C for each fixed S, with only mild curvature at the extremes.

At any fixed temperature, ν increases with dissolved solids S, consistent with the reduced fraction of free water and stronger solute–solvent interactions. The magnitude of this concentration effect is temperature-dependent: at 20 °C, increasing S from 12→15 % raises ν\nuv by 0.16 mm²/s for "Golden Rangers" (1.46 → 1.62) and by 0.16 mm²/s for "Simirenko" (1.42 → 1.58); at 40 °C, the rise is 0.14 (GR: 1.28 → 1.42) and 0.15 (Sim: 1.23 → 1.38); at 80 °C, the increment is smaller—0.09 (GR: 0.85 → 0.94) and 0.10 (Sim: 0.83 → 0.93). Thus, the sensitivity to S attenuates with increasing t, indicating partial compensation of concentration-induced structuring by thermal disruption of the liquid microstructure.

A cultivar effect is present across the entire domain: at identical (t,S), "Golden Rangers" is slightly more viscous than "Simirenko," typically by 0.02–0.05 mm²/s. This offset is largest at lower temperatures and higher S (e.g., 30 °C, S = 14%: 1.54 vs 1.48 mm²/s) and tends to diminish at higher temperatures and lower S (e.g., 80 °C, S = 13%: 0.88 vs 0.87 mm²/s), which aligns with modest compositional differences between cultivars (sugar/acid ratio, pectin/colloid content). Taken together, the data define a coherent picture: temperature lowers ν in a near-linear fashion, dissolved solids raise ν with a strength that wanes as t increases, and cultivar-specific composition introduces a small, stable upward shift for "Golden Rangers."

Effect of temperature and dissolved solids on thermal conductivity

The thermal conductivity (λ) of apple juice was studied in relation to both temperature and the mass fraction of dissolved solids. Measurements were carried

out for three concentrations of dissolved solids -12%, 13%, and 15% (w/w) - within the temperature range of 20 °C to 90 °C. The obtained results are shown in Figures 2-4.

As can be seen from the graphs, thermal conductivity increases with rising temperature regardless of dissolved solids content. For the juice sample containing 12% solids, the thermal conductivity coefficient increased by approximately 21.1% over the studied temperature range. For the samples with 13% and 15% solids, the corresponding increases were 20.4% and 18.7%, respectively.

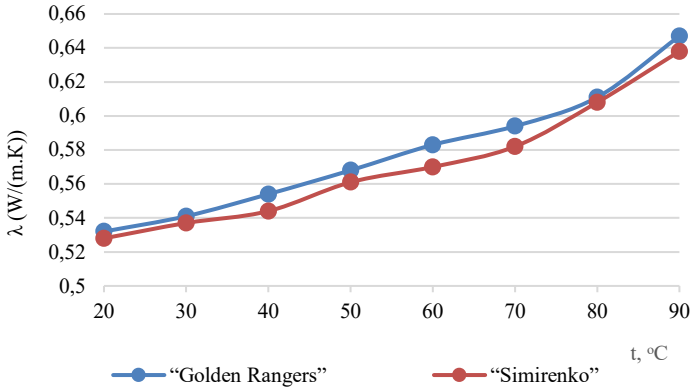

Figure 2 Temperature dependence of thermal conductivity (λ, W m⁻¹ K⁻¹) of apple juice containing 12% (w/w) dissolved solids

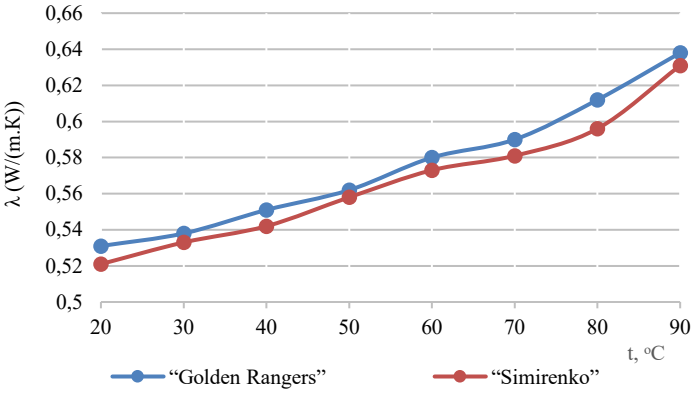

Figure 3 Temperature dependence of thermal conductivity (λ, W m⁻¹ K⁻¹) of apple juice containing 13% (w/w) dissolved solids

At the same time, an increase in the concentration of dissolved solids from 12% to 15% leads to a moderate reduction in thermal conductivity at a given temperature. On average, the decrease is approximately 3.2%. This behavior can be attributed to the influence of dissolved substances such as sugars, which limit the mobility of water molecules and thereby reduce the efficiency of heat transfer through the liquid medium.

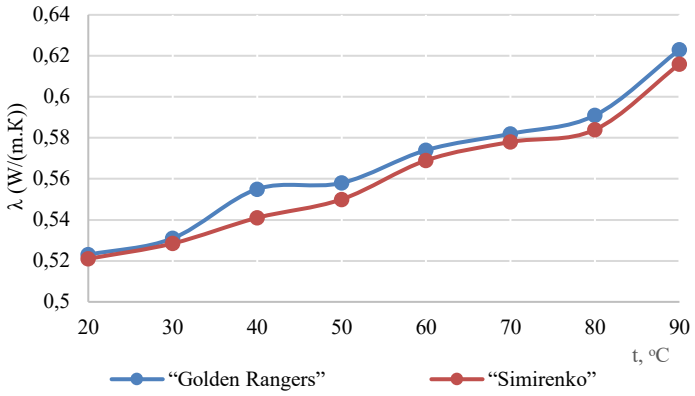

Figure 4 Temperature dependence of thermal conductivity (λ, W m⁻¹ K⁻¹) of apple juice containing 15% (w/w) dissolved solids

Temperature-dependent variation in specific heat capacity

The specific heat capacity (C_p, kJ·kg⁻¹·K⁻¹) of the juice samples was calculated using Equations (5) - (7), based on both the mass fraction of dissolved solids and temperature. The results for the "Golden Rangers" and "Semirenko" apple varieties are summarized in (Tab 4).

Table 4 Temperature-dependent variation in the specific heat capacity of juice samples

Temperature (°C)	**Heat capacity (C_p, kJ·kg⁻¹·K⁻¹)**							
	"Golden Rangers"				"Semerenko"			
	Mass fraction of dissolved solids (%)							
	12	**13**	**14**	**15**	**12**	**13**	**14**	**15**
20	3,754	3,762	3,77	3,778	3,627	3,634	3,641	3,648
30	3,774	3,782	3,79	3,798	3,654	3,661	3,668	3,675
40	3,794	3,802	3,81	3,818	3,681	3,688	3,695	3,702
50	3,815	3,823	3,831	3,839	3,708	3,715	3,722	3,729
60	3,835	3,843	3,851	3,859	3,735	3,742	3,749	3,756
70	3,854	3,862	3,87	3,878	3,762	3,769	3,776	3,783
80	3,875	3,883	3,891	3,899	3,789	3,796	3,803	3,81
90	3,895	3,903	3,911	3,919	3,816	3,823	3,83	3,837

The table 4 shows a steady, near-linear increase of C_p (kJ·kg⁻¹·K⁻¹) with temperature t across 20–90 °C at closely similar mass fractions of dissolved solids S (12–15%). For "Golden Rangers," at each fixed S the total increment over 20→90 °C is essentially constant at ≈0.141 kJ·kg⁻¹·K⁻¹ (e.g., S = 13%: 3.762 → 3.903 kJ·kg⁻¹·K⁻¹; S = 12%: 3.754 → 3.895; S = 15%: 3.778 → 3.919), corresponding to an average temperature sensitivity of about 0.020 kJ·kg⁻¹·K⁻¹ per 10 °C. For "Simirenko," the rise is somewhat larger: the total increment is ≈ 0.189 kJ·kg⁻¹·K⁻¹ (e.g., S=13%: 3.634 → 3.823; S = 12%: 3.627 → 3.816; S = 15%: 3.648 → 3.837), i.e., about 0.027 kJ·kg⁻¹·K⁻¹ per 10 °C. Against this background, the effect of S within the narrow 12–15% window appears as a small but reproducible upward shift: for "Golden Rangers," the difference between 12% and 15% at any temperature is ≈ 0.024 kJ·kg⁻¹·K⁻¹ (e.g., 20 °C: 3.754 → 3.778; 90 °C: 3.895 → 3.919); for "Simirenko," it is ≈ 0.021 (20 °C: 3.627 → 3.648; 90 °C: 3.816 → 3.837), equivalent to roughly 0.007–0.008 kJ·kg⁻¹·K⁻¹ per 1% solids and markedly smaller than the temperature effect. At identical (t,S) points, "Golden Rangers" exhibits systematically higher C_p than "Simirenko," but the inter-cultivar gap narrows as temperature increases (e.g., at 20 °C and S=12%: 3.754 vs 3.627; at 90 °C: 3.895 vs 3.816; the difference contracts from ~0.127 to ~0.079 kJ·kg⁻¹·K⁻¹, consistent with the stronger temperature sensitivity of "Simirenko" In relative terms at S=13%, the 20→90 °C increase corresponds to ≈3.7% for "Golden Rangers" (3.762 → 3.903) and ≈5.2% for "Simirenko" (3.634 → 3.823). Even these seemingly moderate percentages are operationally significant: a higher C_p implies a greater heat load to raise product temperature, which is critical for pasteurization and thermal stabilization regimes, thermal balances, energy consumption, and equipment sizing. Accounting for cultivar specificity and the weak but systematic influence of S enables more accurate heat-load predictions and optimization of the energy efficiency of processing operations.

Nomograms for operational determination of thermo-physical properties of juice

In the management of thermal and mechanical processes in the food industry, accurate knowledge of the thermo-physical properties of raw materials and semi-finished products is essential. Rapid determination of these properties under production conditions enables more efficient control and optimization of technological operations such as pasteurization, mixing, and heat exchange.

To simplify and accelerate the estimation of critical properties, nomograms were developed to represent temperature-dependent variations in density, kinematic viscosity, specific heat capacity, and thermal conductivity of apple juice samples. These graphical tools are particularly useful in field and engineering applications, where fast yet accurate evaluations are required.

The nomograms in Figures 5 and 6 allow simultaneous determination of temperature-dependent density and kinematic viscosity for apple juice with a dissolved-solids content of 13–15% (w/w).

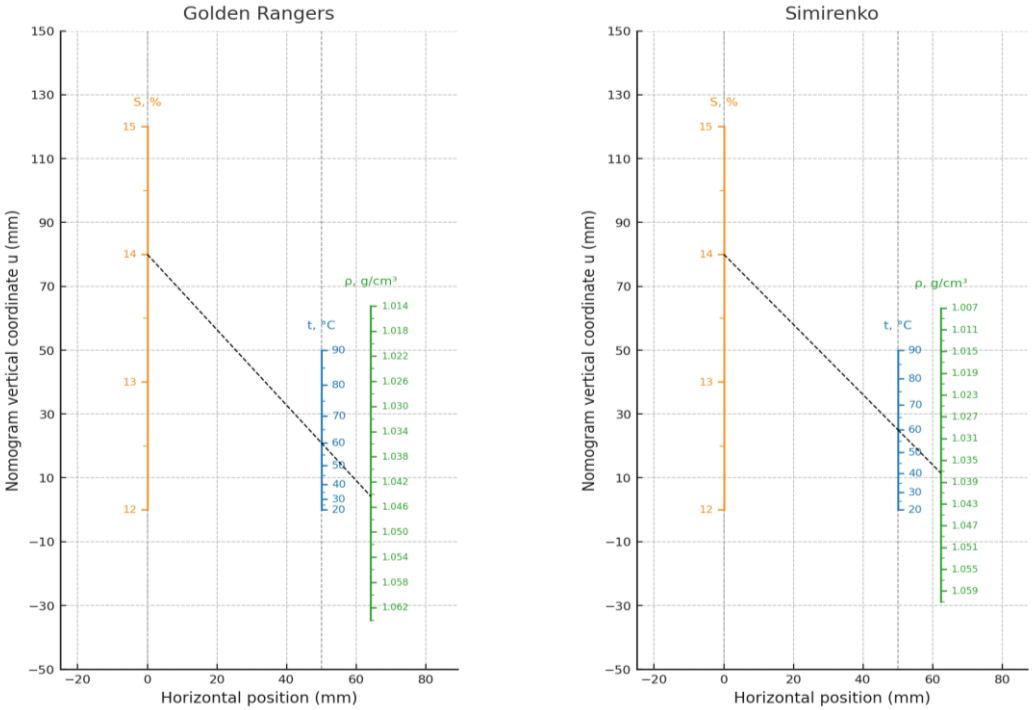

Figure 5 Nomograms for rapid determination of apple juice density *ρ(t,S) – Golden Rangers & Simirenko*

For each cultivar, the density–temperature–soluble-solids relationship was modeled as an additive regression with a mild quadratic curvature in temperature:

$$\rho\ (t,\ S) = a + b{\cdot}t + c{\cdot}S,\ + b_2{\cdot}t^2,$$

where ρ is density (g·cm⁻³), t is temperature (°C), and S is the mass fraction of dissolved solids (%). Cross and quadratic terms in S ($t\ S$, S^2) were tested and found negligible over t=20–90 ∘C and S=12–15%; including t^2 does improve fit (notably for Golden Rangers). Coefficients were estimated by ordinary least squares on the full *(t,S)* grid.

Golden Rangers: $\rho(t,S) = 0.979 + 0.0058 \cdot S - 1.1012 \cdot 10^{-5}t - 4.137 \cdot 10^{-6}t^2\ (g \cdot cm^{-3})$.

Simirenko: $\rho(t,S) = 0.98 + 0.0058 \cdot S - 2.882 \cdot 10^{-4}t - 2.128 \cdot 10^{-6}t^2 (g \cdot cm^{-3})$.

Accuracy is high: for Golden Rangers $R^2 \approx 0.9944$; RMSE =9.44×10^{-4} g·cm⁻³, maximum absolute error = 0.00205 g·cm⁻³; for Simirenko R^2=0.987, RMSE =1.55×10^{-3} g·cm⁻³, maximum absolute error =0.00310 g·cm⁻³. Residuals show no systematic trends in either t or S.

Effects have the expected signs: $\partial\rho/\partial S = c > 0$ (each +1 % in S raises ρ by ≈5.8×10^{-3} g·cm⁻³); $\partial\rho/\partial t = b_1 + 2b_2t < 0$ across 20–90 °C (typical slopes near 60 °C are about -5.1×10^{-4} g·cm⁻³ °C for Golden Rangers and -5.4×10^{-4} for Simirenko).

Because the model is additive, write $\rho - a = f_1(S) + f_2(t)$ with $f_1(S) = c$ and $f_2(t) = b_1t + b_2t^2$, which yields a three-parallel-scale nomogram (left: S; middle: t; right: ρ). Let the visible heights of the S and t scales be H_S and H_T (mm), and the horizontal gap between S and t be H (mm). The vertical scale factors are

$$m = H_S / [c{\cdot}\ (15-12)], \qquad n = H_T / [\max_{20\le t\le 90} f_2(t) - \min_{20\le t\le 90}].$$

(choose $n < 0$ so that t increases upward when anchored at t=20 ⁰C). With a compact layout (as in the figure), one may set $H_S \approx 240$ mm and $H_t \approx 120$ mm, i.e., H=*50 mm*, the scale equations (vertical coordinate u in mm; x_S=*0*, x_T=H, x_ρ= m H /(m+n) are

S-scale: $x = x_S$, $u = m{\cdot}\ [c{\cdot}\ (S - 12)]$

t-scale: $x = x_T$, $u = n{\cdot}\ [f_2(t) - f_2(20)]$

ρ-scale: $x = x_\rho$, $u = (m{\cdot}n)/\ (m + n)\ {\cdot}\ [\ (\rho - a) - (c{\cdot}12 + f_2(20))]$

Numerically, this gives:

Golden Rangers: Δf_2=0.032625⇒m=240/(0.005775·3)=13852.81 mm, n=120/0.032625=−,678.16 mm, x_ρ≈68.1 mm, and (mn)/(m+n) =−5,007.82 mm·(g·cm⁻³)⁻¹.

Simirenko: Δf_2=0.0365625⇒m=240/(0.0057875·3)=13,822.89 mm, n=120/0.0365625=−3,282.05 mm, x_ρ≈65.6 mm, and (mn)/(m+n) =−4,303.97 mm·(g·cm⁻³)⁻¹.

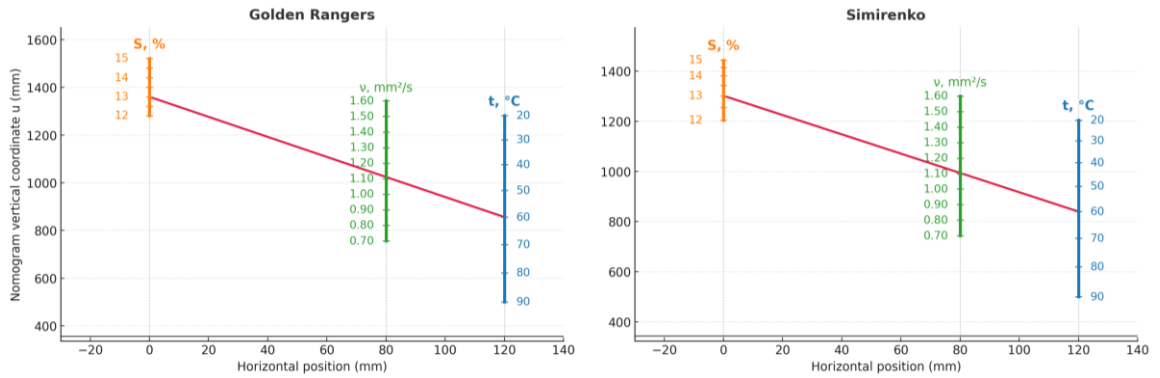

Figure 6 Nomograms for rapid determination of apple juice kinematic viscosity *v(t,S)– Golden Rangers & Simirenko*

Recommended tick ranges are S=12,12.5,…,15%; t=20,25,…,90 ^{0}C; and $\rho \approx$ 1.00-1.07 g·cm^{-3} with 0.002–0.004 spacing. A straight indicator line through $(x_S,u_S(S))$ and $(x_T,u_T(t))$ intersects the density scale at (x_ρ,u_ρ), yielding ρ with graphical reading errors (≈±0.2 mm) on the order of 4-5×10^{-5} g·cm^{-3}, i.e., well below the regression RMSE. Inverse lookups (solve for t or S given ρ and the other factor) use the same construction.

Kinematic viscosity $\nu(t,S)$, thermal conductivity $\lambda(t,S)$, and specific heat capacity $C_p(t,S)$ are handled analogously: for each cultivar, coefficients of a quadratic (or-where diagnostics justify-linear) regression are estimated by least squares on the full (t,S) grid; models are checked by R^2, RMSE and residual analysis; and the additive form Y-a=$f_1(t)$+$f_2(S)$ is used to construct three-parallel-scale nomograms with unified vertical coordinates. The regression equations for ν, λ, and C_p for both cultivars will be presented together with their fit metrics in the Results section and can be inserted into the same nomographic framework without altering the plotting algorithm.

Both cultivars display consistent trends: at fixed S viscosity decreases monotonically with temperature t, while at fixed t it increases with dissolved solids S. Quadratic regressions describe the data with high accuracy:

Golden Rangers: $\nu(t,S)=1.267-0.00945t+0.0324S-1.7708\cdot10^{-5}t^2+3.125\cdot10^{-4}S^2$
$R^2=0.9924$.
Simirenko: $\nu(t,S)=0.239-0.00709t+0.1696S-3.4077\cdot10^{-5}t^2-4.687\cdot10^{-3}S^2$
$R^2=0.9959$.

These R^2 values indicate that the models explain ~99.2–99.6% of the observed variance, adequate for engineering use and nomogram readout.

Figures 7 and 8 present nomograms that enable the determination of specific heat capacity (C_p) and thermal conductivity (λ) across the temperature range relevant to industrial thermal processing.

Nomograms of thermal conductivity for *Golden Rangers* and *Simirenko* apple juices were constructed using an additive, non-interaction polynomial model of the form $\lambda(t,S)=b_0+f_2(t)+f_1(S)$, where $f_2(t)=\sum_{k=1}^{4}\alpha_k t^k$ and $f_1(S)=\sum_{k=1}^{4}\gamma_k S^k$. This separable specification (without the interaction term t,S) implements the relation $f_3=f_1+f_2$ and enables a three-parallel-scale nomogram (left S, center λ, right t) in which the desired value is obtained by a single straight line connecting the chosen S and t. The approximation was fitted to the experimental grid t=20–90 ^{0}C, S=12–15%; the equations used in the nomograms are:

Golden Rangers for:
$\lambda(t,S)=10^{-2}-6.5\cdot10^{-3}t+2.6\cdot10^{-4}t^2-3.6\cdot10^{-6}t^3+1.8\cdot10^{-8}t^4+0.036S+0.012S^2-0.0015S^3+4.4\cdot10^{-5}$
(goodness of fit: $R^2=0.9902$, RMSE =3.32·10^{-3} W/(m·K), max|Δ|=0.0099);
Simirenko for:
$\lambda(t,S)=5.2\cdot10^{-2}-6.8\cdot10^{-3}t+2.6\cdot10^{-4}t^2-3.5\cdot10^{-6}t^3+1.7\cdot10^{-8}t^4+0.17S-0.02S^2+0.001S^3-1.8\cdot10^{-5}S$
(goodness of fit: $R^2=0.9934$ RMSE=0.00269 W/(m·K),max|Δ|=0.00594).

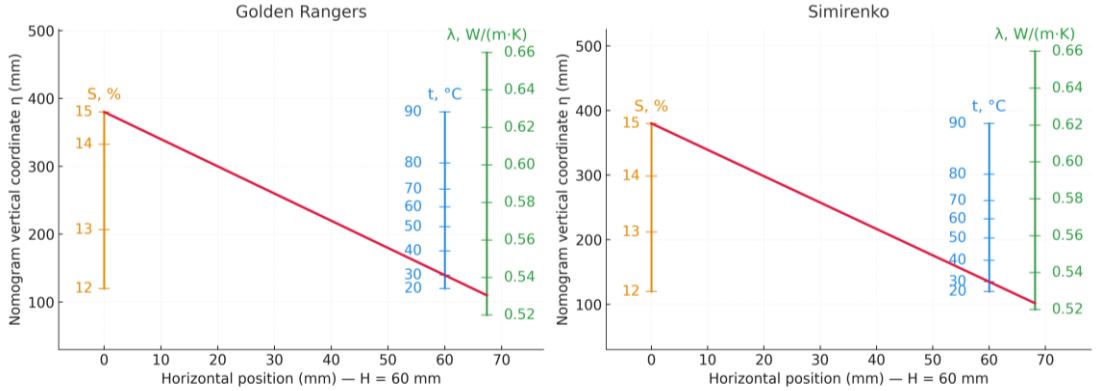

Figure 7 Nomograms for rapid determination of apple juice thermal conductivity λ *(t,S)– Golden Rangers & Simirenko*

Within these domains the nomograms reproduce the expected thermophysical trends - λ increases monotonically with temperature and, on average, decreases with increasing dissolved-solids content; at identical *(t,S)* conditions, *Golden Rangers* typically exhibits slightly higher λ than *Simirenko*, consistent with compositional differences. Reading is straightforward: a straight line through the selected S and t intersects the central scale at λ; use outside the calibration ranges is not recommended.

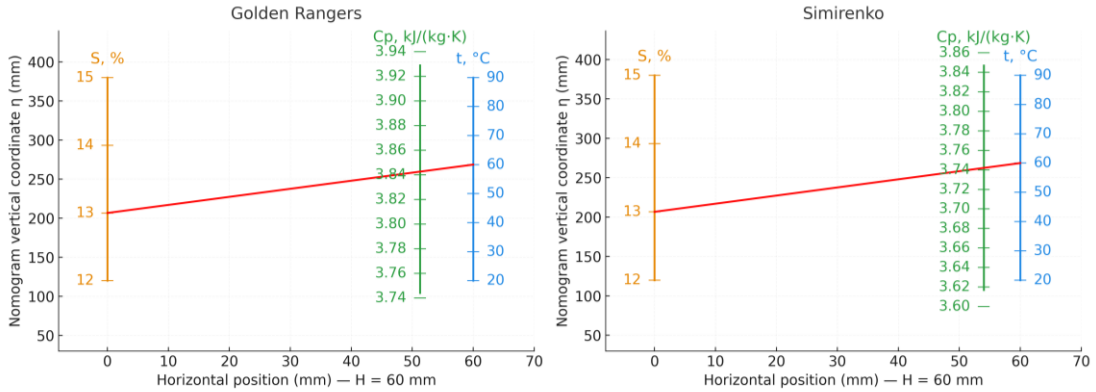

Figure 8 Nomograms for rapid determination of apple juice heat capacity C_p *(t,S)– Golden Rangers & Simirenko*

The regression was fitted on the grid t = 20–90^{0}C, S = 12–15% using a two-factor linear approximation:

Golden Rangers: C_p=3.617714+0.002014 t+0.008 S,
Simirenko: C_p=3.489+0.0027 t+0.007 S.

Within this range the data are reproduced essentially exactly ($R^2\rightarrow1$; RMSE on the order of 10^{-4} kJ·kg^{-1}·K^{-1}), which is sufficient for engineering calculations of thermal loads and energy balances.

The coefficients reveal cultivar-specific behavior: Simirenko shows a stronger temperature response (+2.7×10^{-3} kJ·kg^{-1}·K^{-1} per 1 °C vs. +2.014×10^{-3} for Golden Rangers), whereas the effect of dissolved solids is slightly larger for Golden Rangers (+0.0080 vs. +0.0070 kJ·kg^{-1}·K^{-1} per 1 % S). Consequently, at equal t and S the C_p of Golden Rangers is usually marginally higher, while the increase with temperature is more pronounced for Simirenko. These trends are consistent with compositional differences (sugar–acid ratio and colloidal fraction) that influence the heat capacity of aqueous sugar systems.

The nomograms enable rapid, calculation-free reading: selecting t and S on the outer scales yields C_p on the central scale; inverse lookups are analogous. Use is recommended within the calibration bounds; outside them, additional nonlinearity checks are warranted.

These nomograms offer a convenient tool for engineers and technologists, facilitating the design and control of heat transfer systems with minimal computational effort. Their accuracy has been verified against calculated values and experimental data, confirming their suitability for practical use in juice processing environments.

CONCLUSION

We analyzed single-strength apple juices of two cultivars - *Golden Rangers* and *Simirenko* - with soluble-solids concentrations of 12.7–14.3% (11.5–13 °Brix), consistent with literature for single-strength juices. Across 20–90 °C, we identified cultivar-specific additive regressions and constructed three parallel-scale nomograms for density ρ, kinematic viscosity ν, thermal conductivity λ, and specific heat capacity c_p. The models reproduce the tabulated values with engineering accuracy; for density, typical RMSE is on the order of 10^{-3} g·cm^{-3} with maximum absolute errors of 2 - 3×10^{-3}g·cm^{-3}, and residuals show no systematic trends in temperature or solids. The corresponding nomograms enable rapid, transparent, computation-free reading of each property and support inverse look-ups (solving for t or S given a target property value).

Uncertainty analysis indicates that the dominant contributors are measurement error in the underlying property and temperature control together with specimen variability; the graphical reading error of the nomograms (≈±0.2 mm) is an order of magnitude smaller than the regression error and therefore not limiting. In practical terms, the tools address industrial needs (on-line quality checks, set-up of heating/blending regimes, quick mass/energy estimates), modelling (fast approximations and sanity checks that can be embedded via the reported equations), and education (visualizing joint effects of temperature and composition and training in graphical calculation). Compared with purely computational workflows, nomograms offer transparency, immediacy, and offline use, while the fitted equations integrate seamlessly into digital environments; together they are complementary.

The workflow - experimental grid acquisition, OLS fitting of additive models, and translation into three-scale nomograms -is transferable to additional fruits and broader solids ranges. Although the present dataset covers two cultivars within a single-strength interval, the methodology scales directly; extending the cultivar set and solids span will strengthen external validity and broaden applicability. Practically, we provide printable nomograms and closed-form equations for ρ, ν, λ, and c_p over 20 - 90 °C for the two cultivars, enabling fast and reproducible property estimates for industrial, modelling, and educational use.

REFERENCES

Bagde, N. I., & Tumane, P. M. (2011). Studies on microbial flora of fruit juices and cold drinks. Asiatic Journal of Biotechnology Resources, 2(4), 454–460.

Gestal, M., Andrade, J. M., Dorado, J., Fernández, E., & Prada, D. (2004). Classification of apple beverages using artificial neural networks with previous variable selection. Analytica Chimica Acta, 524(1–2), 225–234. https://doi.org/10.1016/j.aca.2004.02.030

Mullen, W., Marks, S. C., & Crozier, A. (2007). Evaluation of phenolic compounds in commercial fruit juices and fruit drinks. Journal of Agricultural and Food Chemistry, 55(8), 3148–3157. https://doi.org/10.1021/jf062970x

Agbaje, R. B., Ibrahim, T. A., & Raimi, O. T. (2020). Physico-chemical properties and sensory qualities of juices extracted from five selected fruits and their peels. International Journal of Engineering Applied Sciences and Technology, 4(11), 239–244. https://doi.org/10.33564/IJEAST.2020.v04i11.041

Salehi, F. (2020). Physicochemical characteristics and rheological behavior of some fruit juices and their concentrates. Journal of Food Measurement and Characterization, 14, 2472–2488. https://doi.org/10.1007/s11694-020-00495-0

Evrendilek, G. A., Jin, Z., Ruhlman, K. T., Qiu, X., Zhang, Q., & Richter, E. R. (2000). Microbial safety and shelf-life of apple juice and cider processed by bench and pilot scale PEF systems. Innovative Food Science & Emerging Technologies, 1(1), 77–86. https://doi.org/10.1016/S1466-8564(99)00004-1

Deniskin, V. V., & Gorelova, T. P. (2004). Consumption of juice products in European countries. Pivo i Napitki, (5), 8–10.

Goren'kov, E. S., & Magerramov, M. A. (2006). Thermophysical properties of juices from subtropical fruits. Pivo i Napitki, (2), 56–59.

Makarova, N. V., & Valiulina, D. F. (2012). Comparative analysis of physicochemical properties and antioxidant activity of apple juices. Pivo i Napitki, (5), 50–52.

Erdogdu, F. (2005). Mathematical approaches for use of analytical solutions in experimental determination of heat and mass transfer parameters. Journal of Food Engineering, 68(2), 233–238. https://doi.org/10.1016/j.jfoodeng.2004.05.038

Walkling-Ribeiro, M., Noci, F., Cronin, D. A., Riener, J., Lyng, J. G., & Morgan, D. J. (2008). Reduction of Staphylococcus aureus and quality changes in apple juice processed by ultraviolet irradiation, pre-heating, and pulsed electric fields. Journal of Food Engineering, 89(3), 267–273. https://doi.org/10.1016/j.jfoodeng.2008.05.001

Bayindirli, L. (1992). Mathematical analysis of variation of density and viscosity of apple juice with temperature and concentration. Journal of Food Processing and Preservation, 16(1), 23–28. https://doi.org/10.1111/j.1745-4549.1992.tb00190.x

Magerramov, M. A., Abdulagatov, A. I., Azizov, N. D., & Abdulagatov, I. M. (2007). Viscosity of tangerine and lemon juices as a function of temperature and concentration. International Journal of Food Science and Technology, 42(7), 804–818. https://doi.org/10.1111/j.1365-2621.2007.01286.x

Gasperi, F., Aprea, E., Biasioli, F., Carlin, S., Endrizzi, I., Pirretti, G., & Spilimbergo, S. (2009). Effects of supercritical CO_2 and N_2O pasteurisation on the quality of fresh apple juice. Food Chemistry, 115(1), 129–136. https://doi.org/10.1016/j.foodchem.2008.11.078

Magerramov, M. A. (2006). [Thermal conductivity of fruit juices in forced flow]. Izvestiya VUZov. Pishchevaya Tekhnologiya, (5), 46–50.

G'anijonov, D. I., & Ismailov, O. Y. (2025). [Study of the effect of temperature on the kinematic viscosity and heat capacity of freshly squeezed fruit juices]. Uzbek Journal of Agricultural Science, (3), 117–121.

G'anijonov, D. I., & Ismailov, O. Y. (2025). [Investigation of physical properties of direct-pressed juices for optimizing heat and hydrodynamic processes]. Universum: Tekhnicheskie Nauki, 58–61. https://7universum.com/ru/tech/archive/item/19333

Ganijonov, D. I., Ismailov, O. Y., Karomova, F. I., Pirimov, T. J., & Nurmukhamedov, A. A. (2024). Energy of heat exchanger devices increase efficiency. Science and Education in Karakalpakstan, 4, 242–247.